Basic Study of Iterative Learning Control Using Basis Functions for Various Tasks of a Ball-screw-driven Stage

Takumi HAYASHI[*a)] Student Member, Hiroshi FUJIMOTO[*] Senior Member
Yoshihiro ISAOKA[**] Non-member, Yuki TERADA[**] Non-member

Ball-screw-driven stages are positioning systems widely used in industrial equipment such as numerically controlled machine tools. High-precision and high-speed position control is required but difficult due to rolling friction in ball-screw mechanism. Iterative learning control (ILC) is one of the effective control methods for friction compensation, but its industrial application is limited because of the vulnerability to task variation (*e.g.* position reference variation). To handle various tasks, projection-based ILC using basis functions is proposed in conventional studies. In this paper, basis functions for position control of ball-screw-driven stages are proposed based on the physical properties of ball-screw-driven stages including rolling friction. Simulations and experiments validate our proposal's effectiveness.

Keywords: Iterative learning control, projection-based iterative learning control, ball-screw-driven stage, rolling friction.

1. Introduction

Ball-screw-driven stages, as shown in Fig. 1, are positioning systems which convert motor's rotational motion into stage's translational motion. They are widely used in industrial equipment such as numerically controlled (NC) machine tools. In NC machine tools, precise and fast machining is required for high production quality and throughput. Therefore, high-precision and high-speed position control of ball-screw-driven stages is necessary.

However, high-precision position control of ball-screw-driven stages is difficult due to their nonlinear friction, called rolling friction. The characteristics of rolling friction are divided into two regions, region 1 and region 2, as shown in Fig. 2. In region 1, rolling friction has nonlinearity and depends on relative position from stage's velocity reversal points. In region 2, rolling friction shows Coulomb friction T_c which is almost constant. Because of the nonlinearity in region 1, it is well known that large tracking error arises near stage's velocity reversal points.

Various studies have been conducted to compensate rolling friction. The compensation methods are classified into two types, model-based methods and learning-based methods. In model-based methods, various models of rolling friction have been proposed, *e.g.* LuGre model [1], Generalized Maxwell Slip model [2], Rheology-based model [3]. These model-based methods require the precise measurement of rolling friction and the parameter tuning of the complex friction models. Rolling friction can be compensated if the parameters are well tuned. However, the parameter tuning is time-consuming and rolling friction is not able to be compensated perfectly because rolling friction depends on environment and operating condition.

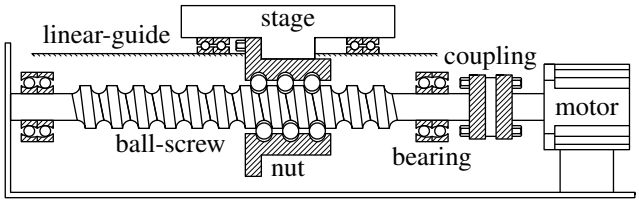

Fig. 1. Schematic view of ball-screw-driven stages.

This paper considers learning-based compensation [4]. In learning-based methods, rolling friction is compensated by iterative learning under the assumption that the same task is repeated. Iterative learning control (ILC) [5, 6] is one of the learning-based control methods. However, standard ILC (S-ILC) has a disadvantage that re-learning is required after the task changes. To solve this problem, recently studies on ILC using basis functions called projection-based ILC (P-ILC) have been conducted [7, 8]. In P-ILC, basis functions are used to handle various tasks. However, rolling friction compensation is not considered in previous studies on P-ILC. Therefore, in this paper, P-ILC using new basis functions with consideration of rolling friction compensation is proposed. Its effectiveness is demonstrated through simulations and experiments.

This paper is organized as follows. First, experimental setup is described in Section 2, and Section 3 introduces ILC and P-ILC. Simulations and experiments are conducted in Section 5 and Section 6 to demonstrate our proposal's effectiveness. Finally, Section 7 presents conclusion and future work.

2. Experimental setup

2.1 Modeling The experimental setup used in this paper is depicted in Fig. 3. This experimental setup has two

a) Correspondence to: hayashi.takumi18@ae.k.u-tokyo.ac.jp
* The University of Tokyo
5-1-5, Kashiwanoha, Kashiwa, Chiba, 277-8561 Japan
** DMG MORI CO., LTD.
362, Idono, Yamatokoriyama, Nara, 639-1183 Japan

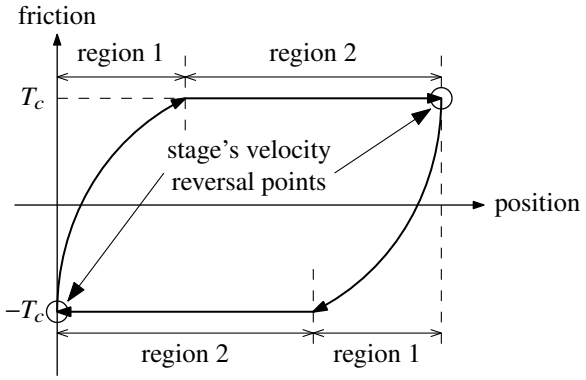

Fig. 2. Characteristics of rolling friction of ball-screw–driven stages.

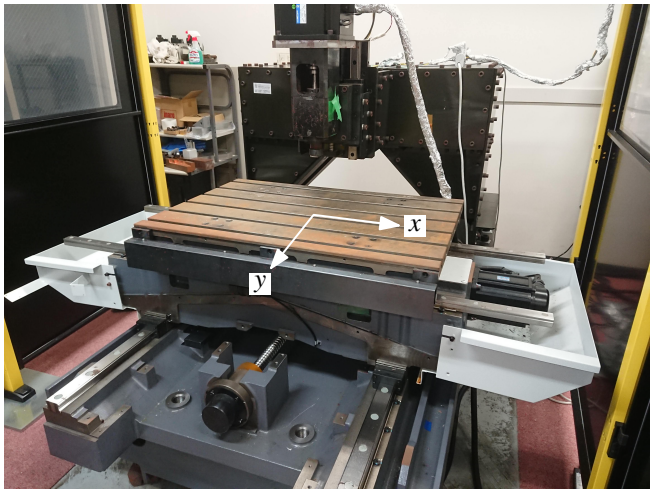

Fig. 3. Picture of the experimental setup.

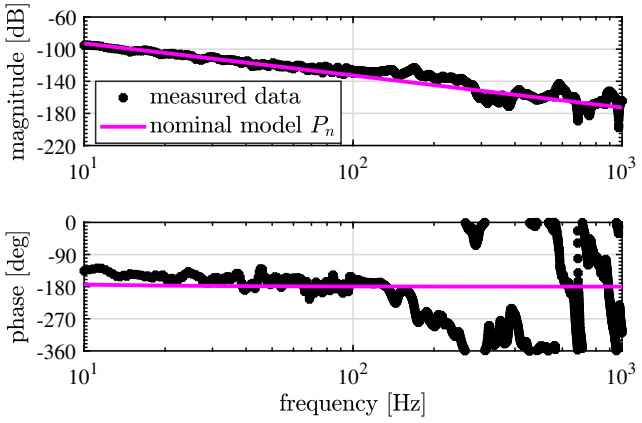

Fig. 4. Frequency response from motor's current i [A] to stage's position x [m] of x-axis of the experimental setup.

axes, x-axis and y-axis. Only x-axis is used in this paper. Figure 4 shows the frequency response data from motor's current i [A] to stage's position x [m] of x-axis measured by frequency domain identification [9]. In this paper, only rigid mode is considered and the nominal model of this experimental setup is expressed as follows:

$$P_n(s) = \frac{x}{i} = \frac{RK_T}{J_n s^2 + D_n s} \cdots\cdots (1)$$

Table 1. Parameters of the experimental setup.

Nominal inertia J_n	0.015 kgm^2
Nominal viscosity coefficient D_n	0.1 N m s rad^{-1}
Torque constant K_T	0.715 N m A^{-1}
Ball-screw's lead R	1.91 mm rad^{-1}

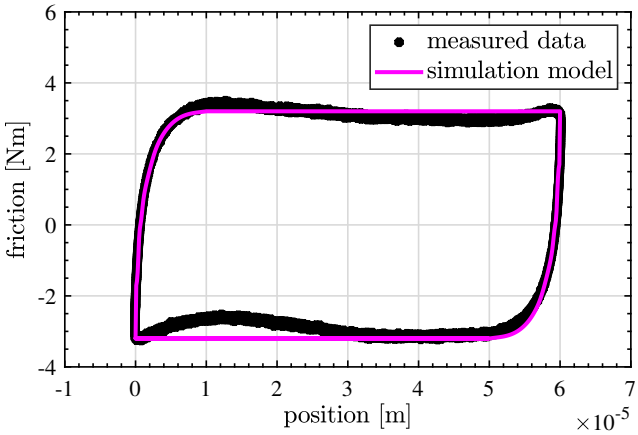

Fig. 5. Rolling friction of the experimental setup.

Parameters in (1) are shown in Table 1.

2.2 Rolling Friction Rolling friction of the experimental setup is shown in Fig. 5. This data is measured by ultra-low speed examination and disturbance observer. According to Fig. 5, the range of region 1 and Coulomb friction T_c in Fig. 2 are identified to be 10 µm and 3.2 N m, respectively.

Note that the "simulation model" in Fig. 5 is only used in the simulation referred in Section 5 and not used for any controller design.

3. Iterative Learning Control

3.1 Lifted System Representation ILC is one of the learning-based control methods and becomes effective if the same task is repeated. By repeating the same task and updating feedforward input from previous trial's error, tracking error is gradually suppressed.

In this paper, lifted system representation [10] is used to analyze ILC. A time-series signal of ILC's one trial is expressed as

$$\boldsymbol{x} = \begin{bmatrix} x[0] & x[1] & \cdots & x[N-1] \end{bmatrix}^\top \in \mathbb{R}^N, \cdots\cdots (2a)$$
$$x[i] = x(iT_s), \cdots\cdots (2b)$$

where N is the length of one trial and T_s is the sampling time. The convolution matrix $\mathcal{G}$ of a discrete-time linear time-invariant system $G[z]$ is represented as follows:

$$\mathcal{G} = \begin{bmatrix} g_0 & 0 & \cdots & 0 \\ g_1 & g_0 & \cdots & 0 \\ \vdots & \vdots & \ddots & 0 \\ g_{N-1} & g_{N-2} & \cdots & g_0 \end{bmatrix} \in \mathbb{R}^{N\times N}, \cdots\cdots (3)$$

where g_i ($i = 0, 1, \ldots, N-1$) denotes the impulse response coefficient:

$$G[z] = g_0 + g_1 z^{-1} + \cdots + g_{N-1} z^{-(N-1)} \cdots\cdots (4)$$

By using lifted system representation, the relation between

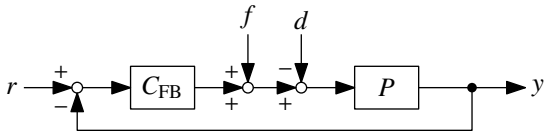

Fig. 6. Block diagram of two-degree-of-freedom control system (r: reference, y: output, P: linear time invariant system, C_{FB}: feedback controller, f: feedforward input, d: disturbance).

input u and output y of system G is given by

$$\boldsymbol{y} = \mathcal{G}\boldsymbol{u}, \quad \cdots (5a)$$

$$\boldsymbol{u} = \begin{bmatrix} u[0] & u[1] & \cdots & u[N-1] \end{bmatrix}^\top, \quad \cdots (5b)$$

$$\boldsymbol{y} = \begin{bmatrix} y[0] & y[1] & \cdots & y[N-1] \end{bmatrix}^\top. \quad \cdots (5c)$$

3.2 Tracking Error Suppression by Iterative Learning Control Consider the two-degree-of-freedom control system as shown in Fig. 6. In Fig. 6, tracking error e is given by

$$e = r - y = Sr - SP(f - d), \quad \cdots (6)$$

where S is sensitivity function:

$$S = \frac{1}{1 + C_{\mathrm{FB}}P}. \quad \cdots (7)$$

In the jth trial of ILC, by using lifted system representation, (6) can be rewritten as

$$\boldsymbol{e}_j = \mathcal{S}\boldsymbol{r}_j - \mathcal{S}\mathcal{P}\left(\boldsymbol{f}_j - \boldsymbol{d}_j\right). \quad \cdots (8)$$

Here, subscript j denotes the number of trial. In ILC, next trial's feedforward input $\boldsymbol{f}_{j+1}$ is generated from $\boldsymbol{f}_j$ and $\boldsymbol{e}_j$ as follows:

$$\boldsymbol{f}_{j+1} = \mathcal{Q}\left(\boldsymbol{f}_j + \mathcal{L}\boldsymbol{e}_j\right). \quad \cdots (9)$$

$\mathcal{L}$ and $\mathcal{Q}$ are the convolution matrices corresponding to the learning filter and Q filter, respectively. From (8) and (9), next trial's tracking error $\boldsymbol{e}_{j+1}$ is expressed as

$$\begin{aligned} \boldsymbol{e}_{j+1} &= \mathcal{S}\boldsymbol{r}_{j+1} - \mathcal{S}\mathcal{P}\left(\boldsymbol{f}_{j+1} - \boldsymbol{d}_{j+1}\right) \\ &= \mathcal{Q}(\boldsymbol{I} - \mathcal{S}\mathcal{P}\mathcal{L})\boldsymbol{e}_j + (\boldsymbol{I} - \mathcal{Q})(\mathcal{S}\boldsymbol{r} - \mathcal{S}\mathcal{P}\boldsymbol{d}) \quad \cdots (10) \end{aligned}$$

with the assumption that reference $\boldsymbol{r}$ and disturbance $\boldsymbol{d}$ are the same in all trials:

$$\boldsymbol{r}_1 = \boldsymbol{r}_2 = \cdots =: \boldsymbol{r}, \quad \cdots (11a)$$

$$\boldsymbol{d}_1 = \boldsymbol{d}_2 = \cdots =: \boldsymbol{d}. \quad \cdots (11b)$$

From the recurrence formula (10), tracking error of ILC monotonically decreases when (12) is satisfied.

$$\max\{|\rho\{\mathcal{Q}(\boldsymbol{I} - \mathcal{S}\mathcal{P}\mathcal{L})\}|\} < 1 \quad \cdots (12)$$

Here, $\rho\{\boldsymbol{A}\}$ denotes an eigenvalue of matrix $\boldsymbol{A}$.

Design methods of the two filters L, Q are referred in [5].

4. Iterative Learning Control for Various Tasks

S-ILC is an effective method when the reference $\boldsymbol{r}$ is precisely repeated, but it has a problem that re-learning is required after the reference changes. In order to overcome this problem, studies on P-ILC have been conducted.

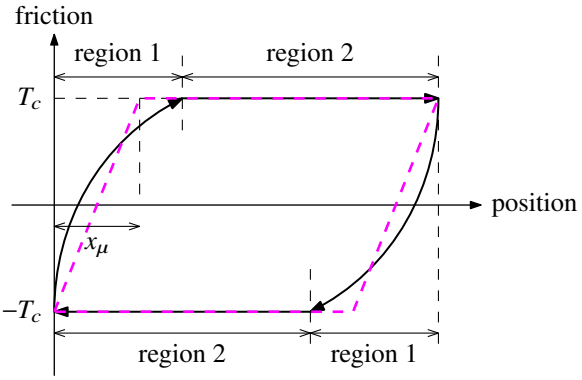

Fig. 7. Real characteristics (black solid line) and approximation (magenta dashed line) of rolling friction.

In the jth trial of P-ILC, the feedforward input $\boldsymbol{f}_j^p$ is parameterized as follows:

$$\boldsymbol{f}_j^p = \boldsymbol{\Psi}\left(\boldsymbol{r}_j\right)\boldsymbol{\theta}_j, \quad \cdots (13a)$$

$$\boldsymbol{\Psi}\left(\boldsymbol{r}_j\right) \in \mathbb{R}^{N \times n_\theta}, \quad \cdots (13b)$$

$$\boldsymbol{\theta}_j \in \mathbb{R}^{n_\theta}, \quad \cdots (13c)$$

where $\boldsymbol{\Psi}\left(\boldsymbol{r}_j\right)$ is the basis functions depending on the jth trial's reference $\boldsymbol{r}_j$, and $\boldsymbol{\theta}_j$ is the parameters independent of $\boldsymbol{r}_j$ but depending on the plant P, respectively. Subscript p implies "P-ILC".

4.1 Selection of Basis Functions

4.1.1 Conventinal Basis Functions From (6), when no disturbance exists ($d = 0$), feedforward input f to follow output y to reference r is expressed as

$$f = P^{-1}r \Rightarrow e = 0. \quad \cdots (14)$$

Considering the ball-screw-driven stages' transfer function $P = RK_T/\left(Js^2 + Ds\right)$, (14) can be rewritten as follows:

$$f = \frac{J}{RK_T}\ddot{r} + \frac{D}{RK_T}\dot{r}. \quad \cdots (15)$$

Thus, the basis functions $\boldsymbol{\Psi}\left(\boldsymbol{r}_j\right)$ and the parameters $\boldsymbol{\theta}_j$ of the jth trial are determined as follows:

$$\boldsymbol{\Psi}\left(\boldsymbol{r}_j\right) = \begin{bmatrix} \ddot{r}[0] & \dot{r}[0] \\ \ddot{r}[1] & \dot{r}[1] \\ \vdots & \vdots \\ \ddot{r}[N-1] & \dot{r}[N-1] \end{bmatrix}, \quad \cdots (16a)$$

$$\boldsymbol{\theta}_j = \begin{bmatrix} J/RK_T & D/RK_T \end{bmatrix}^\top. \quad \cdots (16b)$$

In P-ILC, plant's parameters J/RK_T and D/RK_T are estimated in each trial.

4.1.2 Proposed Basis Functions for Rolling Friction Compensation In order to control ball-screw-driven stages precisely, rolling friction should be compensated. To consider rolling friction in P-ILC, it is approximated as shown in Fig. 7 to make the optimization problem easy in the next subsection. Rolling friction d is expressed as

$$\begin{aligned} d &\approx \mathrm{sign}(\dot{r}) \cdot \min\left(\frac{2T_c}{x_\mu}x_r - T_c,\ T_c\right) \\ &= T_c \cdot \mathrm{sign}(\dot{r}) \min\left(\frac{2}{x_\mu}x_r - 1,\ 1\right) \end{aligned}$$

$$= T_c \cdot \mathrm{Fric}(t), \quad (17)$$

where

$$\mathrm{Fric}(t) \coloneqq \mathrm{sign}(\dot{r}) \min\left(\frac{2}{x_\mu} x_r - 1,\ 1\right). \quad (18)$$

Here, x_μ is a free parameter and x_r is a relative position from stage's velocity reversal point, respectively. In this paper, it is assumed that data of rolling friction as shown in Fig. 5 has already been obtained and x_μ is designed based on the measured data. Therefore, it is assumed that only T_c is variable depending on environment and operating condition in this paper. In the proposed P-ILC, Fric(t) is a part of $\boldsymbol{\Psi}(\boldsymbol{r}_j)$ and Coulomb friction T_c is a part of $\boldsymbol{\theta}_j$.

From the above discussion, the proposed basis functions $\boldsymbol{\Psi}(\boldsymbol{r}_j)$ and the parameters $\boldsymbol{\theta}_j$ are determined as follows:

$$\boldsymbol{\Psi}(\boldsymbol{r}_j) = \begin{bmatrix} \ddot{r}[0] & \dot{r}[0] & \mathrm{Fric}[0] \\ \ddot{r}[1] & \dot{r}[1] & \mathrm{Fric}[1] \\ \vdots & \vdots & \vdots \\ \ddot{r}[N-1] & \dot{r}[N-1] & \mathrm{Fric}[N-1] \end{bmatrix}, \quad (19a)$$

$$\boldsymbol{\theta}_j = \begin{bmatrix} J/RK_T & D/RK_T & T_c \end{bmatrix}^\top. \quad (19b)$$

4.2 Parameter Estimation To estimate parameters $\boldsymbol{\theta}_{j+1}$ of the $(j+1)$th trial of P-ILC, an optimization problem is presented. In S-ILC, tracking error of the $(j+1)$th trial is expressed from (8) as follows:

$$\boldsymbol{e}_{j+1} = \mathcal{S}\boldsymbol{r}_{j+1} - \mathcal{SP}\left(\boldsymbol{f}_{j+1} - \boldsymbol{d}_{j+1}\right). \quad (20)$$

By assuming that $\boldsymbol{r}_{j+1} = \boldsymbol{r}_j$ and $\boldsymbol{d}_{j+1} = \boldsymbol{d}_j$, $\boldsymbol{e}_{j+1}$ can be predicted as (21) from (8) and (20) by using nominal plant before the $(j+1)$th trial is done.

$$\hat{\boldsymbol{e}}_{j+1} = \boldsymbol{e}_j - \mathcal{S}_n\mathcal{P}_n\left(\boldsymbol{f}_{j+1} - \boldsymbol{f}_j\right), \quad (21)$$

where $\hat{\boldsymbol{e}}_{j+1}$ is the predicted tracking error and subscript n denotes the nominal plant's value. In the same way, predicted tracking error $\hat{\boldsymbol{e}}^p_{j+1}$ of P-ILC's $(j+1)$th trial is given by

$$\hat{\boldsymbol{e}}^p_{j+1} = \boldsymbol{e}_j - \mathcal{S}_n\mathcal{P}_n\left(\boldsymbol{\Psi}(\boldsymbol{r}_j)\boldsymbol{\theta}_{j+1} - \boldsymbol{f}_j\right). \quad (22)$$

Here, $\boldsymbol{\Psi}(\boldsymbol{r}_j)\boldsymbol{\theta}_{j+1}$ is the feedforward input calculated when $\boldsymbol{r}_{j+1} = \boldsymbol{r}_j$ and $\boldsymbol{d}_{j+1} = \boldsymbol{d}_j$.

In this paper, the optimization problem

$$\min_{\boldsymbol{\theta}_{j+1}} \left\| \hat{\boldsymbol{e}}_{j+1} - \hat{\boldsymbol{e}}^p_{j+1} \right\|_2 \quad (23a)$$

$$\Rightarrow \min_{\boldsymbol{\theta}_{j+1}} \left\| \mathcal{S}_n\mathcal{P}_n\boldsymbol{f}_{j+1} - \mathcal{S}_n\mathcal{P}_n\boldsymbol{\Psi}(\boldsymbol{r}_j)\boldsymbol{\theta}_{j+1} \right\|_2 \quad (23b)$$

is solved by the least-square method to determine $\boldsymbol{\theta}_{j+1}$ [7]. Note that the analytical solution of $\boldsymbol{\theta}_{j+1}$ can be obtained under the assumption that the matrix $\mathcal{S}_n\mathcal{P}_n\boldsymbol{\Psi}(\boldsymbol{r}_j)$ is nonsingular, *i.e.* the reference $\boldsymbol{r}_j$ is a persistently-exciting signal.

Finally, reference is updated to $\boldsymbol{r}_{j+1}$ and feedforward input is calculated as

$$\boldsymbol{f}^p_{j+1} = \boldsymbol{\Psi}(\boldsymbol{r}_{j+1})\boldsymbol{\theta}_{j+1}. \quad (24)$$

Then, $(j+1)$th trial is done.

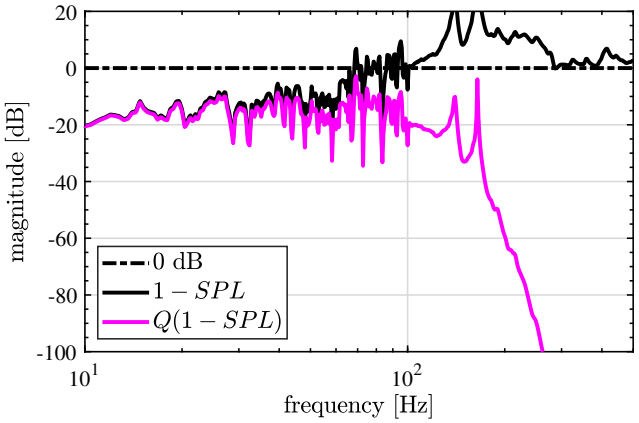

Fig. 8. Bode diagram of $1 - S\,LP$ and $Q(1 - S\,LP)$.

5. Simulation

To verify effectiveness of the proposed P-ILC using basis functions for rolling friction compensation, simulations are conducted and S-ILC, the conventional P-ILC using the basis functions (16) (Conv. P-ILC), and the proposed P-ILC using the basis functions (19) (Prop. P-ILC) are compared. Here, sampling time T_s is set to 1 ms.

5.1 Condition

5.1.1 Plant In the simulations, the nominal plant and simulation plant are the same as shown in Fig. 4. Therefore, modeling error is not considered in the simulation.

Rolling friction used in the simulations is shown in Fig. 5. The range of the region showing nonlinearity is 10 µm and Coulomb Friction T_c is 3.2 N m.

5.1.2 Feedback Controller Feedback controller C_{FB} is a PID controller designed to have 30 Hz closed loop multiple poles by the pole placement method. It is discretized by the Tustin transformation with sampling time $T_s = 1$ ms.

5.1.3 Learning Filter and Q Filter Learning filter L is designed by ZPETC algorithm [11] and Q filter Q is N_Qth-order zero-phase low-pass filter.

$$Q(z) = \left(\frac{z + 2 + z^{-1}}{4}\right)^{N_Q}. \quad (25)$$

$Q(z)$ is realized by $Q_r(z)$ with N_Q samples delay compensation of the memory.

$$Q_r(z) = Q(z) \cdot z^{-N_Q}. \quad (26)$$

In frequency domain, ILC's convergence condition (12) denotes that gain of $Q(1 - S\,LP)$ is less than 0 dB at all frequencies.

$$\max\left\{\left|Q(\mathrm{j}\omega)(1 - S(\mathrm{j}\omega)L(\mathrm{j}\omega)P(\mathrm{j}\omega))\right|\right\} < 0\,\mathrm{dB}. \quad (27)$$

Figure 8 shows the gain of $1 - S\,LP$ and $Q(1 - S\,LP)$. N_Q is set to 24 to satisfy (27).

5.1.4 Position References and Basis Functions Figure 9 shows two types of position references. First, r_1 is used until the 5th trial of ILC. From the 6th trial, reference changes to r_2 to compare S-ILC and P-ILC from the perspective of robustness against position reference variation.

From the position references shown in Fig. 9, basis functions of P-ILC are given as Fig. 10. Here, x_μ is set to 5 µm.

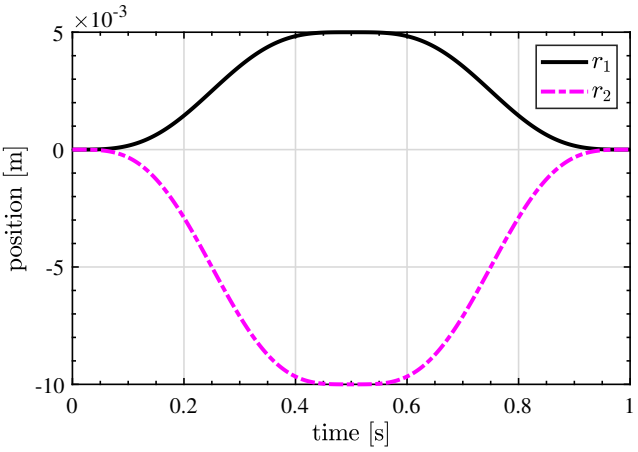

Fig. 9. Position references.

5.2 Results The simulation results are shown in Fig. 11, demonstrating effectiveness of the proposed P-ILC. Figures 11(a) and 11(b) show Root-Mean-Square (RMS) error E_j^{RMS} and maximum error E_j^{MAX} of the jth trial, respectively. E_j^{RMS} is defined as follows:

$$E_j^{\mathrm{RMS}} := \sqrt{\frac{\|\boldsymbol{e}_j\|_2^2}{N}} \quad \cdots\cdots (28)$$

The other figures of Fig. 11 show the tracking error and feedforward input of one trial before and after the position reference variation.

5.2.1 Comparison between Conventinal P-ILC and Proposed P-ILC According to Fig. 11, it can be said that the tracking error drastically decreases by using basis functions for rolling friction compensation (19). The effectiveness of the proposed P-ILC is demonstrated.

5.2.2 Comparison between Standard ILC and Proposed P-ILC According to the tracking error and feedforward input after the position reference variation, shown in Figs. 11(d) and 11(f), it can be said that the proposed P-ILC is robust against position reference variation, while S-ILC cannot handle position reference variation. However, S-ILC is better from the viewpoint of tracking error after learning precisely repeated reference, see the tracking error of the 5th trial shown in Figs 11(a), 11(b), and 11(c). The causes of the proposed P-ILC's larger tracking error after finishing learning can be considered as follows:

- Selection of basis functions: Basis functions are determined based on continuous-time systems. But in the real world, systems are discretized by zero-order hold (ZOH). Therefore, for more precise control, basis functions are determined based on systems with ZOH.
- Approximation of rolling friction: To consider rolling friction in P-ILC, it is approximated as shown in Fig. 7. Therefore, mismatch exists between the real rolling friction and its approximation model used in the proposed P-ILC.

6. Experiment

Experiments are conducted to verify the effectiveness of the proposed P-ILC. Experimental condition is the same as that of simulation.

The experimental results are shown in Fig. 12 and show the same tendency as the simulation. However, the performance of the proposed P-ILC deteriorates compared to that in the simulations. It can be considered that this deterioration is caused by the modeling error of the experimental setup. For more precise control of ball-screw-driven stages, high-order resonance should be considered. To consider high-order resonance in P-ILC, basis functions should consist of high-order derivatives of position reference, *e.g.* jerk and snap.

7. Conclusion and Future Work

To control ball-screw-driven stages precisely, rolling friction should be compensated. The compensation methods are classified into two types, model-based and learning-based methods. S-ILC is one of the learning-based methods. However, S-ILC can handle only precisely repeated task, and deteriorates when the task changes. To overcome this problem, recently studies on P-ILC have been conducted. P-ILC can handle various tasks by using basis functions. However, rolling friction compensation is not considered in previous studies on P-ILC. Therefore, in this paper, P-ILC using the basis functions for rolling friction compensation is proposed. Simulations and experiments demonstrate that the proposed P-ILC can suppress tracking error greatly compared with the conventional P-ILC without consideration of rolling friction compensation. For more precise control of ball-screw-driven stages based on P-ILC, selection of basis functions and approximation of rolling friction are considered in future works.

References

(1) C. Canudas de Wit, H. Olsson, K. Astrom, and P. Lischinsky, "A New Model for Control of Systems with Friction," *IEEE Transactions on Automatic Control*, vol. 40, no. 3, pp. 419–425, 1995.

(2) F. Al-Bender, V. Lampaert, and J. Swevers, "The Generalized Maxwell-Slip Model: A Novel Model for Friction Simulation and Compensation," *IEEE Transactions on Automatic Control*, vol. 50, no. 11, pp. 1883–1887, 2005.

(3) Y. Maeda and M. Iwasaki, "Feedforward Friction Compensation Using the Rolling Friction Model for Micrometer-stroke Point-to-point Positioning Motion," *IEEJ Journal of Industry Applications*, vol. 7, no. 2, pp. 141–149, 2017.

(4) H. Fujimoto and T. Takemura, "High-Precision Control of Ball-Screw-Driven Stage Based on Repetitive Control Using n-Times Learning Filter," *IEEE Transactions on Industrial Electronics*, vol. 61, no. 7, pp. 3694–3703, 2014.

(5) D. A. Bristow, M. Tharayil, and A. G. Alleyne, "A Survey of Iterative Learning Control," *IEEE Control Systems*, vol. 26, no. 3, pp. 96–114, 2006.

(6) T. Oomen, "Advanced Motion Control for Precision Mechatronics: Control, Identification, and Learning of Complex Systems," *IEEJ Journal of Industry Applications*, vol. 7, no. 2, pp. 127–140, 2018.

(7) F. Boeren, A. Bareja, T. Kok, and T. Oomen, "Frequency-Domain ILC Approach for Repeating and Varying Tasks: With Application to Semiconductor Bonding Equipment," *IEEE/ASME Transactions on Mechatronics*, vol. 21, no. 6, pp. 2716–2727, 2016.

(8) J. van Zundert, J. Bolder, and T. Oomen, "Optimality and flexibility in Iterative Learning Control for varying tasks," *Automatica*, vol. 67, pp. 295–302, 2016.

(9) R. Pintelon and J. Schoukens, *System Identification: A Frequency Domain Approach*, 2nd ed. Hoboken, NJ, USA: Wiley-IEEE Press, 2012.

(10) T. Chen and B. A. Francis, *Optimal Sampled-Data Control Systems*. Springer, 1995.

(11) M. Tomizuka, "Zero Phase Error Tracking Algorithm for Digital Control," *Journal of Dynamic Systems, Measurement, and Control*, vol. 109, no. 1, pp. 65–68, 1987.

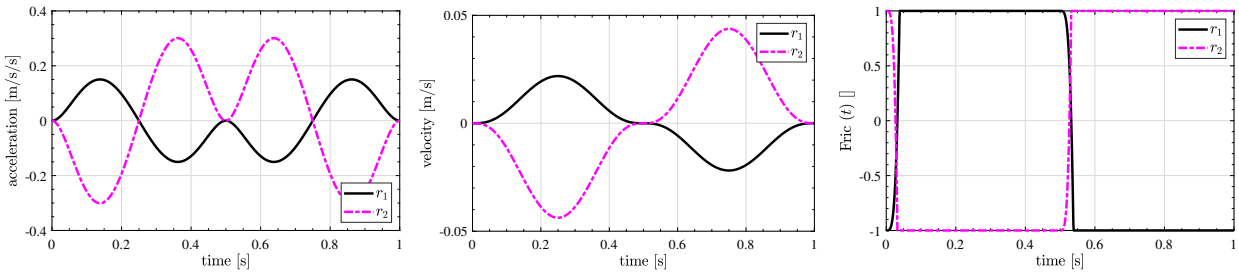

(a) Acceralation. (b) Velocity. (c) Fric(t) defined as (18) (x_μ = 5 µm).

Fig. 10. Basis functions of P-ILC for ball-screw-driven stages.

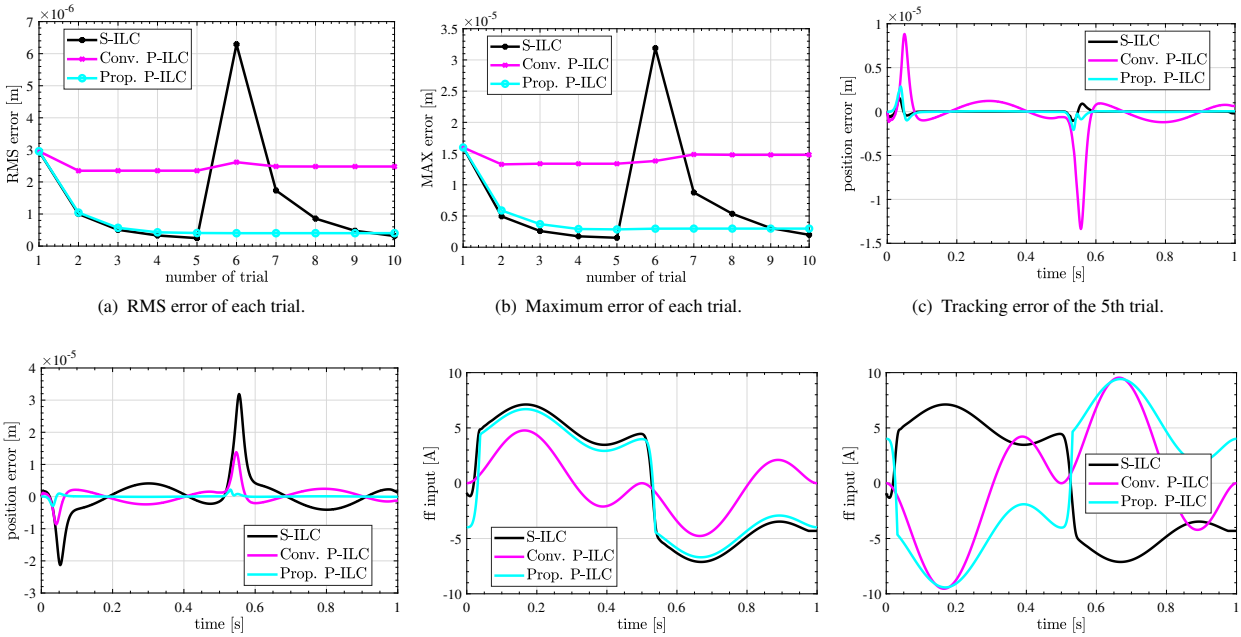

(a) RMS error of each trial. (b) Maximum error of each trial. (c) Tracking error of the 5th trial.

(d) Tracking error of the 6th trial. (e) Feedforward input of the 5th trial. (f) Feedforward input of the 6th trial.

Fig. 11. Simulation results.

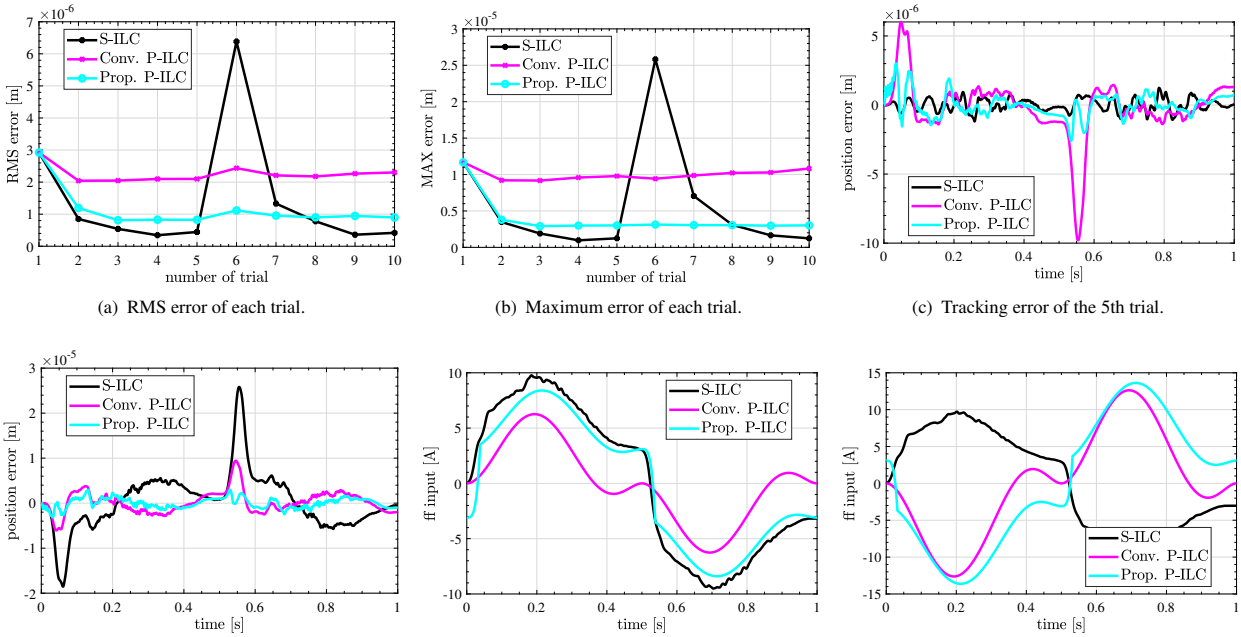

(a) RMS error of each trial. (b) Maximum error of each trial. (c) Tracking error of the 5th trial.

(d) Tracking error of the 6th trial. (e) Feedforward input of the 5th trial. (f) Feedforward input of the 6th trial.

Fig. 12. Experimental results.